American Mineralogist, Volume 92, pages 198–203, 2007

Zincalstibite, a new mineral, and cualstibite: Crystal chemical and structural relationships

Elena Bonaccorsi,* Stefano Merlino, and Paolo Orlandi

Dipartimento di Scienze della Terra, Via S. Maria 53, I-56126 Pisa, Italy

Abstract

Zincalstibite, a new mineral occurring within the cavities of marble of the Apuan Alps, Tuscany, Italy, has chemical formula $Zn_2AlSb(OH)_{12}$, space group $P\bar{3}$, $a = 5.321(1)$, $c = 9.786(2)$ Å. It is associated with sub-millimeter tufts of white crystals of mimetite and sub-millimetric stalactite aggregates of opal and an amorphous copper-silicate phase (possibly crisocolla). The crystals are trigonal prismatic, with forms {110}, {001}, elongated [001], generally less than $10 \times 10 \times 40 \div 50$ μm, with few larger crystals. They are colorless, transparent, with vitreous luster, white streak and {001} cleavage. The stronger reflections are [(*hkl*), *d* (Å), I_{rel}]: (002), 4.904, 100; (100), 4.620, 35; (101), 4.179, 57; (103, 110), 2.669, 31; (112, $11\bar{2}$), 2.343, 88; (114, $11\bar{4}$), 1.805, 57. Zincalstibite is structurally related to cualstibite, as evidenced by the structural determinations and refinements we present for both the minerals. They are built up by layers of isolated $Sb(OH)_6$ octahedra alternating along *c* with trioctahedral layers, which contain Zn and Al cations and Cu and Al cations in zincalstibite and cualstibite, respectively. In cualstibite the ordering of Al and Cu within these trioctahedral layers results in a supercell, with $a_{cual} = 9.150(2)$ Å $\approx \sqrt{3}\, a_{zinc}$. The name of zincalstibite is related to its chemical composition and points to its relationships with cualstibite. Both the mineral and its name were approved by the IMA Commission for New Minerals and Mineral Names (IMA 1998-033).

Keywords: Zincalstibite, cualstibite, new mineral, crystal structure, XRD data

Introduction

Zincalstibite is the fourth mineralogical species, after carraraite, zaccagnaite (Merlino and Orlandi 2001), and möeloite (Orlandi et al. 2002) found, for the first time in nature, within the cavities of marble in the Apuan Alps, Tuscany, Italy. The Apuan Alps are a mountain chain in northern Tuscany running parallel to the Tyrrenian coast for about 60 km, with an average width of about 20 km. They are part of an epizonal metamorphic complex originating from a tertiary Tuscan sedimentary sequence.

A liassic marble formation, composed of very pure limestone having a typical saccharoidal texture, outcrops in this area; its color is white but may contain variable gray and colored banding in places. Marble quarrying in the Apuan Alps began over 2000 years ago, following the Roman conquest of that territory, and expanded with the demand of construction material for public works. The marble from this area is now well known around the world for the constancy of its quality, scarcity of defects, excellent physical and mechanical characteristics, and long-lasting strength and beauty. Nevertheless rare small cavities are also present within some very pure varieties of marble; in these cavities more than 100 mineralogical species, most of which sulfides, have been found (Orlandi and Franzini 1994).

The minerals were deposited from hydrothermal fluids during a space of time of about 6–9 millions of years; the first ones were deposited at a temperature of about 400 °C, the last ones at temperature of about 100 °C or less (Franceschelli et al. 1997). Zincalstibite belongs to this last deposition step and results from the alteration, by aluminum rich hydrothermal fluids, of different sulfides like sphalerite, zinkenite, and stibioluzonite.

* E-mail: elena@dst.unipi.it

Zincalstibite appears closely related to cualstibite, which has been described by Walenta (1984) as a new mineral occurring in trigonal prisms in the secondary assemblage of the Clara Mine near Oberwolfach (Central Black Forest). Very recently, the occurrence of cualstibite has been reported also in two abandoned Italian mines, both situated in the Carnic Alps: Monte Avanza (Forni Avoltri) and Comeglians, Udine province, Friuli-Venezia Giulia, Italy (Ciriotti et al. 2006). The results of the chemical analysis (Walenta 1984; a test for the oxidation state of antimony indicated that it was present as Sb^{5+}) pointed to the following formula: $Cu_6Al_3Sb_3O_{18}\cdot 16H_2O$ or $Cu_6Al_3(SbO_4)_3(OH)_{12}\cdot 10H_2O$. These chemical data are re-interpreted, on the basis of the chemical and structural results obtained for zincalstibite, resulting in the revised chemical formula $Cu_6Al_3Sb_3(OH)_{36}$ or $Cu_2AlSb(OH)_{12}$.

Occurrence and physical, chemical and crystallographic data of zincalstibite

Occurrence and physical properties

Zincalstibite was found in the Lucchetti marble quarry, Fantiscritti marble basin, located near the town of Carrara. The crystals of zincalstibite occur in a small cavity, associated with sub-millimeter tufts of white crystals of mimetite and sub-millimeter stalactite aggregates of opal and an amorphous copper-silicate phase (possibly crisocolla). Zincalstibite appears to have formed as alteration product of different sulfides, sphalerite, zinkenite, stibioluzonite (whose relics were found together with crystals of zincalstibite), through the action of Al-rich hydrothermal fluids.

The crystals are trigonal prismatic, with forms {110}, {001}, elongated [001], generally less than $10 \times 10 \times 40 \div 50$ μm (Fig.

1), with few larger crystals. They are colorless, transparent, with vitreous luster,white streak and {001} cleavage.

Due to the small dimensions of the crystals, their fragility, and mainly due to the presence of encrusting material (opal), the optical properties and the density could not be measured.

X-ray crystallography

Rotation and Weissenberg photographs indicated that the crystals of zincalstibite are trigonal, with cell dimensions a = 5.3, c = 9.8 Å and pointed to space groups $P312$, $P31m$, $P\bar{3}12/m$. Powder diffraction data collected with a Gandolfi camera (diameter 114.6 mm, Cu$K\alpha$ radiation, λ = 1.54178 Å) are presented in Table 1. The indices have been assigned using both the d-values and the values of the intensities collected for the structural study. Both hkl and $hk\bar{l}$ indices, corresponding to non-equivalent reflections with the same d value, are explicitly indicated if both substantially contribute to the intensity of the reflection.

The crystallographic data of zincalstibite compare with those presented by Walenta (1984) for cualstibite: a = 9.20, c = 9.73 Å, in a trigonal or hexagonal space group. Moreover the powder pattern of cualstibite matches very well that of zincalstibite. The main difference between zincalstibite and cualstibite (apart from the presence of zinc in zincalstibite and copper in cualstibite) is the length of the a unit-cell parameter, with $a_{\text{cualstibite}} \approx \sqrt{3}\, a_{\text{zincalstibite}}$ in a unit cell which is related to that of zincalstibite through the transformation matrix [1 $\bar{1}$ 0/1 2 0/0 0 1].

Chemical data

The preliminary qualitative chemical analyses, carried on by means of an EDS spectrometer attached to a Philips 515 Scanning Electron Microscope, pointed to Sb, Zn, and Al as major component with low additional quantities of Cu, Si, and even lower quantities of Fe and S. The actual composition of the mineral was confirmed through microprobe analyses carried out on a wavelength-dispersive Electron Probe JEOL JXA 8600, operating at 10 kV, 2 nA. The pure metallic elements for the four detected components Sb, Zn, Al, and Si were used as standards. The analyses did not show any copper content and indicated that silicon is absent from the structure of zincalstibite. The very small content obtained with the microprobe analyses is due to the contaminating opal phase that encrusts all the crystals.

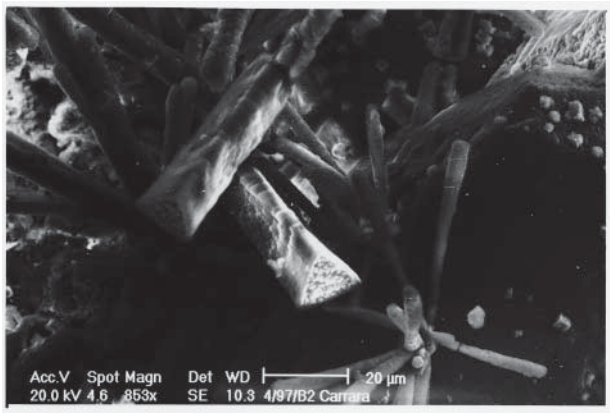

FIGURE 1. SEM image of two crystals of zincalstibite among small sticks of amorphous material.

The analytical data, reported in Table 2, indicated fairly constant contents of Sb_2O_5, ZnO, Al_2O_3, whereas the SiO_2 content was very low and highly variable from point to point. The oxidation state of antimony was suggested by the close relationships of zincalstibite with cualstibite (as it will be indicated in the following) and was fully confirmed by the results of the structural study.

The low sum in the microprobe data, the evident deterioration of the crystals under the electron beam, and the close relationships of zincalstibite with cualstibite indicated a high water content, which was assumed to correspond to the wt% difference of the average total (78.59%) to 100%. The presence of water—actually as hydroxyl groups—has been successively confirmed by the structural study.

Assuming four cations in the unit cell, namely Sb + Zn + Al = 4 (Table 2), we obtained the following empirical formula: $(Zn_{1.90}Al_{1.08}Sb_{1.02})O_{6.05}\cdot 5.7H_2O$.

The name is from the chemical composition of the new natural phase and points to its relationships with cualstibite (Walenta 1984), the corresponding copper, aluminum, antimony hydroxide. The crystal chemical and structural relationships between the two phases will be discussed in a subsequent section.

TABLE 1. X-ray powder pattern of zincalstibite

hkl	d_{calc} (Å)*	d_{obs} (Å)	I_{obs}
002	4.904	4.897	100
100	4.620	4.615	35
101	4.179	4.180	57
102	3.363	3.366	18
103	2.669	2.667	31
110	2.667		
111	2.574	2.573	9
112, 11$\bar{2}$	2.343	2.342	88
201	2.248	2.249	5
104	2.166	2.168	3
202	2.090	2.092	3
113	2.067	2.065	4
203	1.887	1.887	10
105	1.806	1.806	57
114, 11$\bar{4}$	1.805		
211, 211	1.719	1.719	10
204	1.681	1.680	4
212, 21$\bar{2}$	1.644	1.646	4
006	1.635		
300	1.540	1.540	13
302	1.469	1.470	11
116, 11$\bar{6}$	1.393	1.395	11
220	1.334	1.334	6
215, 21$\bar{5}$	1.304	1.303	6
304	1.304		
222, 22$\bar{2}$	1.287	1.286	6

Notes: Gandolfi camera, diameter 114.6 mm, Cu$K\alpha$ radiation, λ = 1.54178 Å.
* The d_{calc} values of zincalstibite have been obtained on the basis of the parameters a = 5.330, c = 9.790 Å.

TABLE 2. Chemical data of zincalstibite (e.s.d. in parenthesis)

Oxide	Average wt%*	Atoms†	Ideal wt%‡
Sb_2O_5	34.12 (2.30)	1.02 (0.07)	33.45
ZnO	32.34 (2.68)	1.90 (0.15)	33.66
Al_2O_3	11.39 (0.62)	1.08 (0.05)	10.54
(SiO_2)	0.74		–
Σ	78.59		
H_2O (diff.)	21.41 (4.83)	5.67 (1.30)	22.35
Σ′	100.00		100.00

* 26 points were analyzed: 21 analytical data were used to calculate the average wt% of Sb_2O_5, ZnO, and Al_2O_3; 5 analytical points with total wt% <70 were not considered.
† Recalculated atomic contents on the basis of (Sb + Zn + Al) = 4.
‡ Theoretical wt% of the oxides for the ideal formula $SbZn_2Al(OH)_{12}$.

The mineral and its name were approved (IMA 98-033) by the Commission on New Minerals and Mineral Names of the International Mineralogical Association.

X-RAY STRUCTURAL STUDY OF ZINCALSTIBITE AND CUALSTIBITE

Experimental methods

Single-crystal diffractometer data. A first collection of X-ray diffraction data was carried out on with a Siemens P4 four-circle diffractometer, operating at 50 kV and 40 mA, with monochromatized Mo$K\alpha$ radiation. Various direct methods runs were performed in the three space groups suggested by the preliminary crystallographic studies, namely $P312$, $P31m$, $P\bar{3}12/m$, and a structural model was found in the $P312$ space group, $a = 5.327(1)$, $c = 9.792(2)$ Å. Although the model could be refined to a final reliability index $R = 0.059$ for 215 reflections with $F_o > 6\sigma(F_o)$, we were not fully convinced of the correctness of the model based on crystal chemical grounds.

To further test this structural model, we carried out a similar data collection and refinement with a crystal of cualstibite from the type locality, kindly given us by Prof. K. Walenta. The diffraction pattern of cualstibite is characterized by a subcell with parameters closely similar to those of zincalstibite [$a = 5.304(2)$, $c = 9.780$ (5) Å]. Only the corresponding subcell reflections were strong enough to be collected and a least-squares refinement was performed in the space group $P312$, starting with the model obtained for zincalstibite and refining the cation occupancies in the various octahedral and trigonal prismatic polyhedra, with a final reliability index $R = 0.059$ for 257 reflections with $F_o > 6\sigma(F_o)$. As in the case of zincalstibite we found oddities in the crystal-chemical features; moreover we did not observed any Jahn Teller distortion in the polyhedra hosting Cu^{2+} cations.

Since the actual unit cell of cualstibite is three times larger than the subcell, we guessed that the oddities in the crystal-chemical features could be solved through the study of the real structure in the larger cell. Moreover we also suspected that in the case of zincalstibite the unsatisfactory crystal-chemical features could be resolved by a trebling of the unit cell.

To measure the very weak superstructure reflections of cualstibite and to check for the possible occurrence of a similar superstructure in zincalstibite, new data were collected for both phases at the Elettra synchrotron facility (Trieste, Italy).

Synchrotron radiation data. The same crystals of cualstibite and zincalstibite previously examined on the 4-circle diffractometer were mounted on the X-ray diffraction beamline XRD1, at the Elettra synchrotron facility (Basovizza-Trieste, Italy). For the cualstibite data collection, the wavelength of the radiation was set to 0.8 Å, and the crystal was placed at the distance of 36 mm from a 165 mm MarCCD detector. The crystal was rotated around the ϕ axis by step of 2°, and 100 frames were recorded and processed with the HKL package of programs (XDISP, DENZO, and SCALEPACK, Otwinowski and Minor 1997), obtaining 6285 reflections. The refined trigonal unit-cell parameters were $a = 9.150(2)$, $c = 9.745(2)$ Å.

The data collection from the crystal of zincalstibite was performed under similar experimental conditions. To obtain information about the possible occurrence of a cualstibite-like superstructure, and because of the weakness of the observed diffraction pattern, the wavelength was set to 1 Å and the exposure time was increased with respect to the collection of the cualstibite data. Moreover, the crystal was rotated by 3° for each frame to obtain enough spots for the auto-indexing process. However, no superstructure reflections were observed in zincalstibite, and the refined trigonal unit cell parameters were $a = 5.321(1)$, $c = 9.786(2)$ Å. The collected frames were processed with the HKL programs (Otwinowski and Minor 1997), obtaining 962 observed reflections. More information concerning both data collection and the subsequent refinements are available in Table 3. An important point to be stressed here is that no superstructure reflections could be observed in zincalstibite, even in long exposed synchrotron radiation X-ray patterns.

Structure determination and refinement

Cualstibite. Models based on the structural results of the preliminary partial refinement were built up in the triple cell, with a corresponding lowering of the symmetry to $P3$, and several refinement cycles were performed with the full set of data. With respect to the incorrect preliminary model, a substantially different polyhedral arrangement emerged from successive Fourier syntheses and refinement cycles, pointing to a structural model characterized by the regular alternation of layers consisting of isolated $Sb(OH)_6$ octahedra and trioctahedral layers with an ordered distribution of Al- and Cu-centered octahedra. The layer of isolated $Sb(OH)_6$ octahedra is very similar to those obtained by Bonazzi and Mazzi (1996) and Friedrich et al. (2000) in their structural studies of bottinoite and brandholzite, respectively. The refinement of the new model was carried out in both space groups $P\bar{3}$ and $P3$; however, no significant improvement was obtained for the lower symmetry model, and consequently $P\bar{3}$ was assumed as the correct space group of cualstibite. After introducing all the oxygen atoms, the refinement in the space group $P\bar{3}$ quickly and smoothly converged. The observed diffraction symmetry $P\bar{3}2/m1$ pointed to possible twinning, the introduction through the TWIN option of SHELXL-97, of a merohedric twinning with [110] as twin axis caused a marked drop in the reliability index and indicated an equal amount of the two twin individuals (Table 3), thus fully justifying the observed diffraction symmetry. A difference Fourier synthesis showed residual maxima in the plane containing the oxygen atoms of the Sb-centered polyhedra, octahedrally distributed around the Sb cations and pointing to the presence—in each twin individual—of a minor amount of $Sb(OH)_6$ octahedra with a different orientation. These maxima (O1A, O3A, O4A) were then introduced as partially occupied oxygen sites in fixed positions and their occupancy was refined under the constraint of the complementary occupancy of O1, O3, O4. The positions of three (H1, H3, H4) of the six independent hydrogen atoms, lying in the $Sb(OH)_6$ octahedra layer, were detected through a final difference Fourier synthesis, whereas three other hydrogen atoms (H2, H5, H6) were placed in position indicated by the O···O hydrogen bonds connecting the two distinct structural layers, as will be discussed later. After introducing anisotropic displacement parameters for all the atoms except H1 to H6 and O1A, O3A, O4A, the final reliability value was $R = 0.047$ for 1024 unique reflections.

The atomic coordinates of cualstibite, together with the isotropic or equivalent displacement factors are reported in Table 4. Tables with anisotropic displacement parameters and the list of F_o and F_c have been deposited.[1]

Zincalstibite. A model was built up, based on the results obtained for cualstibite, consisting of a layer of isolated $Sb(OH)_6$ octahedra at $z = 0$, regularly alternat-

[1] Deposit item AM-07-003, deposit tables with anisotropic displacement parameters and the list of F_o and F_c. Deposit items are available two ways: For a paper copy contact the Business Office of the Mineralogical Society of America (see inside front cover of recent issue) for price information. For an electronic copy visit the MSA web site at http://www.minsocam.org, go to the American Mineralogist Contents, find the table of contents for the specific volume/issue wanted, and then click on the deposit link there.

TABLE 3. Crystal data and structure refinements for cualstibite and zincalstibite

	cualstibite	zincalstibite
Crystal size	0.03 × 0.03 × 0.05 mm³	0.02 × 0.02 × 0.05 mm³
Ideal formula	$Cu_3AlSb(OH)_{12}$	$Zn_2AlSb(OH)_{12}$
Radiation	Synchrotron radiation X-ray beamline XRD1 (Elettra, Trieste, Italy)	
Wavelength	0.8 Å	1.0 Å
Detector	Detector MarCCD 165 mm	
Distance sample-detector	36 mm	36 mm
$\Delta\phi$ (rotation angle for frame)	2°	3°
Space group	$P\bar{3}$	$P\bar{3}$
Unit-cell dimensions	$a = 9.150(2)$ Å $c = 9.745(2)$ Å	$a = 5.321(1)$Å $c = 9.786(2)$ Å
Volume	706.6(3) Å³	239.95(8) Å³
Z	3	1
twin law	[110] as twin axis*	[120] as twin axis*
refined twin fraction	0.498(7)	0.499(12)
θ range	2.9 to 32.2°	2.9 to 32.5°
Index ranges	$-12 \le h \le 12$, $-11 \le k \le 12$, $-11 \le l \le 10$	$-5 \le h \le 5$, $-5 \le k \le 5$, $-9 \le l \le 8$
Reflections collected	6285	962
Independent reflections	1024	204
R(int)	0.035	0.034
Refinement method	Full-matrix least-squares on F^2	
Data/restraints/parameters	1024/0/76	204/0/28
Goodness-of-fit on F^2	1.117	1.386
R indices (all data)	$R1 = 0.0468$, $wR2 = 0.1310$	$R1 = 0.0427$, $wR2 = 0.1107$
Largest diff. peak and hole	1.90 and –0.89 e.Å^{-3}	1.48 and –1.24 e.Å^{-3}

* The twin axis of cualstibite is related to that of zincalstibite by the transformation matrix [1 1 0/1 2 0/0 0 1].

ing with a trioctahedral layer with an ordered distribution of Al- and Zn-centered octahedra located at 0, 0, ½ and ⅓, ⅔, ½, respectively. The refinement carried out in the space group $P\bar{3}$ quickly converged. Also in this case, a lowering of symmetry to *P*3 did not result in any improvement of the refinement, from a crystal chemical point of view. As in the case of cualstibite, introduction of a merohedric twinning (twin axis [120]) caused a marked drop in the reliability index and indicated an equal amount of the two twin individuals. The results of the refinement (more precisely the values of the displacement parameters and the average bond distances for the three cations) pointed to substitutions in the cation sites of the trioctahedral layer; the corresponding populations were established taking into account the chemical data, the electron density at the sites, the charge balance and the average bond distances and were refined in the last refinement cycles. The positions of the two independent hydrogen atoms were detected through a difference Fourier synthesis and were fixed in the final refinement cycles. Anisotropic displacement parameters were refined for Sb, Zn, Al, and O atoms, and the final reliability value was R = 0.043 for 204 unique reflections.

The atomic coordinates of zincalstibite, together with the isotropic or equivalent displacement factors are reported in Table 4. Tables with anisotropic displacement parameters and the list of F_o and F_c have been deposited.

Structure description

Cualstibite. Figure 2 shows the main features of the crystal structure of cualstibite, as seen along [001]: trioctahedral layers built up by Al regular octahedra and Cu distorted octahedra, regularly alternate with layers of isolated regular Sb octahedra. As stated in the previous section, the Sb octahedra may be placed in two different orientations related by reflection in a plane parallel to $(1\bar{2}0)$. As one of the two orientations is largely dominant (~ 90%) we shall constantly refer to it in the following. The bond distances in the various polyhedra are reported in Table 5. The mean bond distances are in good agreement with the values calculated on the basis of effective bond radii (Shannon and Prewitt 1969) [Sb1-O 1.973 Å, Sb2-O 1.971 Å (calculated 1.988 Å); Cu-O 2.077 Å (calculated 2.108 Å); Al1-O 1.905 Å, Al2-O 1.923 Å (calculated 1.908 Å)], which indicates that the atoms are orderly distributed in the cation sites. The $Cu(OH)_6$ polyhedra display the well known Jahn-Teller distortion with four short and two longer Cu-O distances.

The bond valence balance has been calculated with the parameters given by Brese and O'Keeffe (1991). The bond valence sums for the various oxygen atoms are reported in Table 6. The

TABLE 4. Atomic coordinates and equivalent or isotropic displacement parameters (Å²) for cualstibite and zincalstibite

Site	Occupancy	*x*	*y*	*z*	U_{eq}* or U_{iso}
		Cualstibite			
Sb1	1.0	0	0	0	0.0217(3)*
Sb2	1.0	1/3	2/3	0.0034(1)	0.0229(3)*
Cu	1.0	0.6717(1)	0.0095(1)	0.5005(8)	0.0241(3)*
Al1	1.0	0	0	1/2	0.0104(7)*
Al2	1.0	1/3	2/3	0.5045(2)	0.0121(6)*
O1	0.88(1)	0.5190(5)	0.8286(5)	0.1248(5)	0.030(1)*
O2	1.0	0.1172(11)	0.2044(5)	0.6020(4)	0.035(1)*
O3	0.88(1)	0.5035(5)	0.6575(5)	–0.1110(5)	0.028(1)*
O4	0.88(1)	0.0155(5)	–0.1669(5)	–0.1180(5)	0.034(1)*
O5	1.0	0.5415(5)	0.7876(8)	0.4037(4)	0.025(1)*
O6	1.0	0.1261(5)	0.5431(7)	0.6049(4)	0.025(1)*
O1A	0.12(1)	0.829	0.518	0.874	0.04
O3A	0.12(1)	0.658	0.503	0.111	0.04
O4A	0.12(1)	0.833	0.015	0.118	0.04
H1	1.0	0.471	0.901	0.108	0.04
H2	1.0	0.204	0.087	0.294	0.04
H3	1.0	0.579	0.779	–0.085	0.04
H4	1.0	0.741	0.843	0.097	0.04
H5	1.0	0.542	0.789	0.300	0.04
H6	1.0	0.542	0.416	0.292	0.04
		Zincalstibite			
Site	Occupancy	*x*	*y*	*z*	U_{eq}* or U_{iso}
Sb	$Sb_{1.0}$	0	0	0	0.017(1)*
Zn	$Zn_{0.81}Al_{0.19}$	1/3	2/3	0.5002(11)	0.012(1)*
Al	$Al_{0.63}Zn_{0.37}$	0	0	1/2	0.008(2)*
O1	1.0	0.317(3)	0.319(3)	0.3977(5)	0.011(1)*
O2	1.0	–0.137(2)	0.207(2)	–0.1198(11)	0.026(2)*
H1	1.0	0.336	0.348	0.308	0.05
H2	1.0	–0.289	0.186	–0.103	0.05

* U_{eq} is defined as one third of the trace of the orthogonalized U^{ij} tensor.

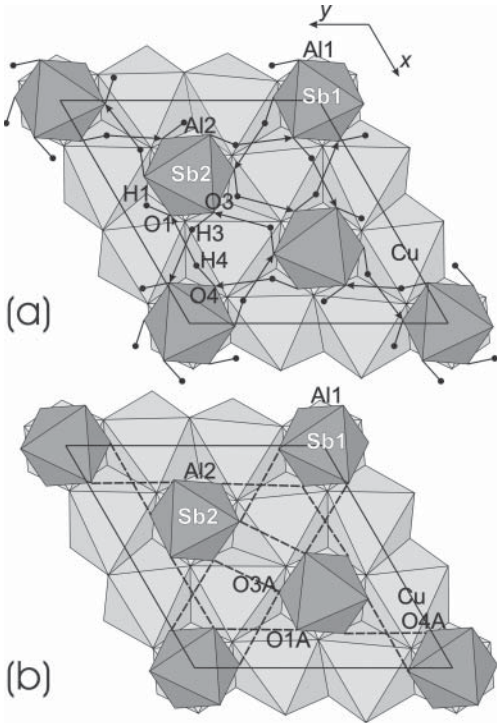

FIGURE 2. Crystal structure of cualstibite as seen down [001]. White and light gray polyhedra correspond to regular aluminum and distorted copper octahedra, respectively, of the trioctahedral layer; the dark gray polyhedra correspond to the isolated $Sb(OH)_6$ octahedra. In **a**, the hydrogen atoms (small black circles) and the hydrogen bonds which interconnect the $Sb(OH)_6$ octahedra within their layer (arrows) are indicated. In **b**, the differently oriented $Sb(OH)_6$ octahedra, which result from the partial occupancy (12%) of the O1A, O3A, and O4A sites, are shown. The dashed lines indicate possible hydrogen bonds within the layer. In both **a** and **b**, the hydrogen bonds between the layers are not reported.

TABLE 5. Bond lengths (Å) for cualstibite (first two columns) and zincalstibite (third and fourth columns)

Cualstibite		Zincalstibite	
Sb1-O4	1.973(4) ×6	Sb-O2	1.982(9) ×6
Sb2-O3	1.951(4) ×3		
-O1	1.991(4) ×3		
Cu-O6	1.928(7)	*Zn-O1	2.068(19) ×3
-O5	2.004(7)	-O1	2.080(20) ×3
-O2	2.012(8)		
-O5	2.094(7)		
-O2	2.158(9)		
-O6	2.263(7)		
Al1-O2	1.905(4) ×6	†Al-O1	1.968(5) ×6
Al2-O6	1.920(4) ×3		
-O5	1.926(4) ×3		

* Site occupancy: $Zn_{0.81}Al_{0.19}$.
† Site occupancy: $Al_{0.63}Zn_{0.37}$.

column Σ_{an} gives the sum of the contributions to each oxygen atom by the various cations: O2, O5, O6—namely the anions of the trioctahedral layer—are heavily overbonded, whereas the anions of the isolated $Sb(OH)_6$ octahedra are underbonded. A reasonable balance is obtained by taking into account the system of hydrogen bonds. Figure 3 illustrates the hydrogen bond system which can be derived from crystal chemical evidence, i.e., (1) position of the hydrogen atoms in the Sb layer; (2) pairs of oxygen atoms with distances lower than 3.0 Å and located in different octahedra; (3) best valence bond balance. The inter-layer hydrogen bonds O2···O4, O5···O1, O6···O3 strongly link the layers of isolated $Sb(OH)_6$ octahedra to the trioctahedral layers, as illustrated in Figure 4, whereas the intra-layer hydrogen bonds O4···O1, O1···O3, O3···O4, illustrated in Figure 2, firmly interconnect the $Sb(OH)_6$ octahedra within the layer. The valence contribution of the various hydrogen bonds have been obtained by applying the equation proposed by Ferraris and Ivaldi (1988) to correlate bond valence vs. H···O distance for the intra-layer hydrogen bonds (for which the positions of the hydrogen atoms have been found) and the equation correlating bond valence vs. O···O distance for the inter-layer hydrogen bonds. The anionic valence bond sums, corrected by taking into account the hydrogen bond system, are reported in the last column of Table 6.

Zincalstibite. The main features of the crystal structure of zincalstibite are quite similar to those already described for cualstibite: layers of isolated Sb octahedra alternate with trioctahedral layers built up by octahedra with dominant Al at 0, 0, ½ and dominant Zn at ⅓, ⅔, ½ (Fig. 5). The bond distances in the octahedra are reported in Table 5; they are in excellent agreement with the values calculated on the basis of effective bond radii (Shannon and Prewitt 1969), after considering the cation distribution in the three independent sites [Sb-O 1.980 Å (calculated 1.988 Å); Zn-O 2.078 Å (calculated 2.082 Å); Al-O 1.970 Å (calculated 1.990 Å)].

The bond valence sums for the two independent oxygen atoms have been calculated taking into account the cation occupancies in the three octahedral sites and are reported in Table 7, column Σ_{an}. The resulting overbonding of O1 and underbonding of O2 are removed (last column of Table 7) through the hydrogen bonding described by Figure 6 and illustrated in Figures 5 and 7.

As in cualstibite, the inter-layer O1···O2 hydrogen bonds link the layers of isolated $Sb(OH)_6$ octahedra to the adjacent trioctahedral layers, whereas the intra-layer hydrogen bonds O2···O2 firmly interconnect the $Sb(OH)_6$ octahedra within the layer. The contribution of the two hydrogen bonds have been obtained by applying the equation proposed by Ferraris and Ivaldi (1988) to correlate bond valence vs. H···O distance

TABLE 6. Bond valence balance for cualstibite (v.u.)

	Sb1	Sb2	Cu	Al1	Al2	Σ_{an}	Σ'_{an}
O1	–	0.876	–	–	–	0.876	1.091*
O2	–	–	0.407 0.274	0.503	–	1.184	0.997†
O3	–	0.976	–	–	–	0.976	1.148*
O4	0.920	–	–	–	–	0.920	1.090*
O5	–	–	0.415 0.326	–	0.476	1.217	1.020†
O6	–	–	0.510 0.206	–	0.483	1.199	1.026†

Notes: Σ_{an} and Σ'_{an} are the sums of the bond strengths for each anion, before and after the correction for the hydrogen bond contributions, respectively.
* The hydrogen bond contributions were calculated on the basis of the observed H···O distance (Ferraris and Ivaldi 1988).
† The hydrogen bond contributions were calculated on the basis of the O···O distance (Ferraris and Ivaldi 1988).

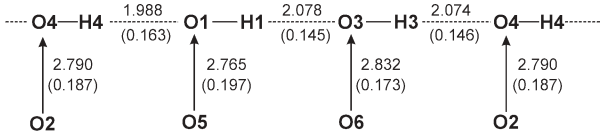

FIGURE 3. Hydrogen bond system in cualstibite. The H···O distance (Å) and the strength of the corresponding hydrogen bond (v.u.) are indicated adjacent to each bond whenever the position of the hydrogen atoms is obtained from Fourier syntheses (H1, H3, H4). The O···O distance (Å) and the strength of the corresponding hydrogen bond (v.u.) are reported for the other three hydrogen bonds. In these cases the arrows point toward the acceptor atom.

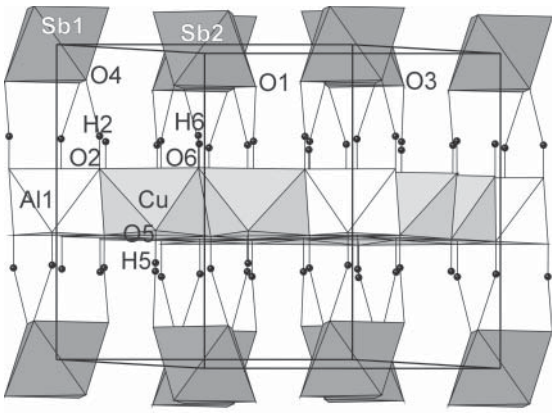

FIGURE 4. Crystal structure of cualstibite as seen down [210] (with a 2° rotation), showing the unit cell. The hydrogen atoms (small black circles) and the hydrogen bonds that connect adjacent layers are indicated. The hydrogen bonds within the $Sb(OH)_6$ layers are not reported here.

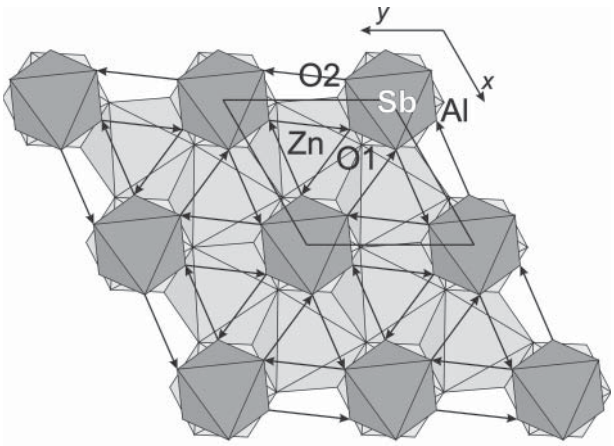

FIGURE 5. Crystal structure of zincalstibite as seen down [001]. White and light gray polyhedra correspond to Al-dominant and Zn-dominant octahedra, respectively, of the trioctahedral layer; the dark gray polyhedra correspond to the isolated $Sb(OH)_6$ octahedra. The dashed lines indicate the hydrogen bonds which interconnect the $Sb(OH)_6$ octahedra within their layer. The hydrogen bonds between the layers are not shown.

TABLE 7. Bond valence balance for zincalstibite (v.u.)

	Sb	Zn	Al	Σ_{an}	Σ'_{an}
O1	–	0.364 0.352	0.450	1.166	0.997*
O2	0.898	–	–	0.898	1.067*

Notes: Σ_{an} and Σ'_{an} are the sums of the bond strengths for each anion, before and after the correction for the hydrogen bond contributions, respectively.
* The hydrogen bond contributions were calculated on the basis of the H···O distance (Ferraris and Ivaldi 1988).

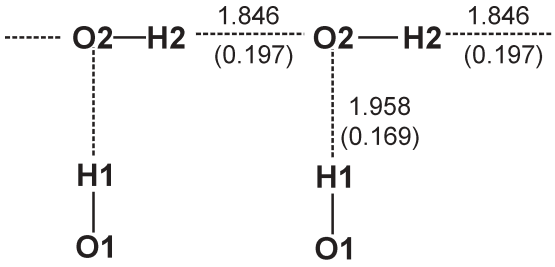

FIGURE 6. Hydrogen bond system in zincalstibite. The H···O distance (Å) and the strength of the corresponding hydrogen bond (v.u.) are indicated adjacent to each bond.

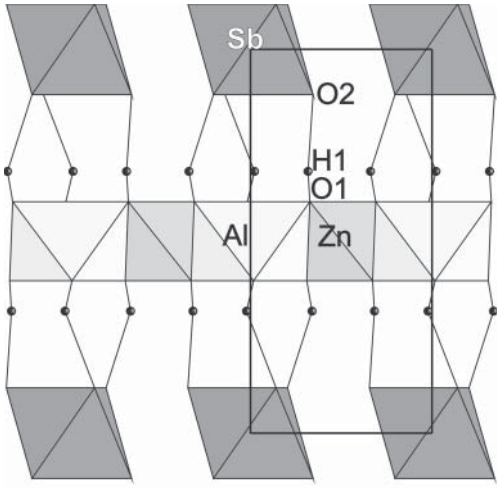

FIGURE 7. Crystal structure of zincalstibite as seen down [100], showing the unit cell. The hydrogen atoms (small black circles) and the hydrogen bonds that connect adjacent layers are indicated. The hydrogen bonds within the layers are not indicated.

DISCUSSION

Cualstibite $Cu_2AlSb(OH)_{12}$ and the new mineral zincalstibite $Zn_2AlSb(OH)_{12}$ display the same structure type, characterized by regularly alternating trioctahedral layers of Cu- (or Zn-) and Al-centered octahedra and layers of isolated $Sb(OH)_6$ octahedra. However the unit cell of cualstibite is three times that of zincalstibite: in fact, whereas only one type of $Sb(OH)_6$ octahedra occurs in zincalstibite, two distinct types exist in cualstibite, one centered at 0, 0, 0 and another at $\frac{1}{3}$, $\frac{2}{3}$, 0 and $\frac{2}{3}$, $\frac{1}{3}$, 0 with opposite orientation. This kind of distribution is most probably connected with the presence, in the trioctahedral layers, of Jahn-Teller distorted Cu octahedra and is required to assure robust hydrogen bonds to firmly link the adjacent layers in the structure.

Layers with $Sb(OH)_6$ octahedra in two distinct orientations have been found in the crystal structures of bottinoite, $Ni(H_2O)_6[Sb(OH)_6]_2$ (Bonazzi and Mazzi 1996), as well as of brandholzite, $Mg(H_2O)_6[Sb(OH)_6]_2$, and corresponding synthetic compounds of Mg and Co (Friedrich et al. 2000). Although the unit net of the $Sb(OH)_6$ layers in those structures is three times that of the $Sb(OH)_6$ layer in cualstibite, the hydrogen bonds which connect the octahedra within the layers follow a unique scheme: "parallel" hydrogen bonds connect iso-oriented octahedra, whereas "crossing" hydrogen bonds connect octahedra with opposite orientation, as illustrated in Figure 1b of Bonazzi and Mazzi (1996).

Zincalstibite and cualstibite differ also in the cation distribution within the trioctahedral layers, which are perfectly ordered in cualstibite and display a substantial degree of disorder in zincalstibite. This feature, too, is related to the Jahn-Teller distortion of the $Cu(OH)_6$ octahedra; due to this distortion they cannot conveniently host aluminum and, at the same time, copper avoids the regular $Al(OH)_6$ octahedron.

ACKNOWLEDGMENTS

The sample of zincalstibite was found by the mineral collector Angelo Simonini, whereas the specimens of cualstibite have been obtained through the kindness of Kurt Walenta; to both of them we are deeply grateful. The microprobe data were collected with a JEOL JXA 8600 electron microprobe at the C.N.R. Centro di Studi per la Minerogenesi e la Geochimica Applicata in Florence with the kind assistance of Dr. Filippo Olmi. The work was supported by MIUR (Ministero dell'Istruzione, dell'Università e della Ricerca) through a grant to the national project "Minerals to materials: crystal chemistry, microstructures, modularity, modulations" and "Systematic mineralogy and crystal-chemistry of minerals of heavy metals." We are grateful to two anonymous referees, whose suggestions and constructive criticism considerably improved the readability of the paper.

REFERENCES CITED

Bonazzi, P. and Mazzi, F. (1996) Bottinoite, $Ni(H_2O)_6[Sb(OH)_6]_2$: Crystal structure, twinning, and hydrogen-bond model. American Mineralogist, 81, 1494–1500.
Brese, N.E. and O'Keeffe, M. (1991) Bond-valence parameters for solids. Acta Crystallographica, B47, 192–197.
Ciriotti, M., Möckel, S., Blaß, G., and Bortolozzi, G. (2006) Cualstibite: ritrovamenti italiani. Micro, 1, 19–24 (in Italian).
Ferraris, G. and Ivaldi, G. (1988) Bond valence vs. bond length in O···O hydrogen bonds. Acta Crystallographica, B44, 341–344.
Franceschelli, M., Memmi, I., Carangiu, G., and Gianelli, G. (1997) Prograde and retrograde chloritoid zoning in low temperature metamorphism, Alpi Apuane, Italy. Schweizerische Mineralogische und Petrographische Mitteilungen, 77, 41–50.
Friedrich, A., Wildner, M., Tillmanns, E., and Merz, P.L. (2000) Crystal chemistry of the new mineral brandholzite, $Mg(H_2O)_6[Sb(OH)_6]_2$, and of the synthetic analogues $M^{2+}(H_2O)_6[Sb(OH)_6]_2$, ($M^{2+}$ = Mg, Co). American Mineralogist, 85, 593–599.
Merlino, S. and Orlandi, P. (2001) Carraraite and zaccagnaite, two new minerals from the Carrara marble quarries: their chemical composition, physical properties and structural features. American Mineralogist, 86, 2222–2244.
Orlandi, P. and Franzini, M. (1994) I minerali del marmo di Carrara. 109 p. Amilcare Pizzi S.p.A., Milano, Italy (in Italian).
Orlandi, P., Meerschaut, A., Palvadeau, P., and Merlino, S. (2002) Lead-antimony sulfosalts from Tuscany (Italy). V. Definition and crystal structure of moeloite, $Pb_6Sb_6S_{14}(S_3)$, a new mineral from the Ceragiola marble quarry. European Journal of Mineralogy, 14, 599–606.
Otwinowski, Z. and Minor, W. (1997) Processing of X-ray Diffraction Data Collected in Oscillation Mode. Methods in Enzymology, 276, 307–326.
Shannon, R.D. and Prewitt, C.T. (1969) Effective ionic radii in oxides and fluorides. Acta Crystallographica, B25, 925–946.
Walenta, K. (1984) Cualstibit, ein neues Sekundarmineral aus der Grube Clara im mittleren Schwarzwald (BRD). Chemie der Erde, 43, 255–260.

MANUSCRIPT RECEIVED FEBRUARY 16, 2006
MANUSCRIPT ACCEPTED AUGUST 7, 2006
MANUSCRIPT HANDLED BY SERGEY KRIVOVICHEV